Article

Not peer-reviewed version

Identifying the Climatic and Anthropogenic Impact on Vegetation Surrounding the Natural Springs of the Arava Valley Using Remote Sensing Methods

Ariel Mordechai Meroz , Avshalom Babad , Noam Levin *

Posted Date: 6 February 2024

doi: 10.20944/preprints202402.0377.v1

Keywords: Drylands; Natural springs; Aquifers; Remote sensing; NDVI

Article

Identifying the Climatic and Anthropogenic Impact on Vegetation Surrounding the Natural Springs of the Arava Valley Using Remote Sensing Methods

Ariel Mordechai Meroz [1,2,*], Avshalom Babad [2] and Noam Levin [1,3]

[1] Department of Geography, Hebrew University of Jerusalem, Mount Scopus, Jerusalem 9190501, Israel.
[2] Dead Sea and Arava Science Center.
[3] Remote Sensing Research Center, School of the Environment, University of Queensland, St Lucia, QLD 4072, Australia.
* Correspondence: ariel.meroz@mail.huji.ac.il.

Abstract: Natural springs, recognized as biodiversity hotspots and keystone ecosystems, exert positive ecological influences beyond their immediate extent, particularly in dryland environments. The water feeding these springs, largely governed by natural climatic conditions, is susceptible to anthropogenic impacts. The objective of this study was to determine the factors that cause fluctuations in water availability to springs of the hyper-arid Arava Valley (Israel/Jordan). Using the Standard Precipitation Index, we statistically classified the historical record of yearly rainfall for the past four decades into clusters of dry and wet sub-periods. We assessed changes in vegetation cover around the springs using the Landsat-derived Normalized Difference Vegetation Index (NDVI) for each sub-period. To assess the anthropogenic effects, we examined the correlations between vegetation cover, water extraction from the aquifer, and the status of adjacent agricultural plots that share a hydrological connection with the springs. Our findings reveal fluctuations between wet and dry sub-periods over the last four decades. We observed high responsiveness of vegetation cover around the springs to these fluctuating sub-periods. Of the 25 studied springs, 12 were directly influenced by anthropogenic factors — seven experienced a decline in vegetation which we attributed to water extraction from the aquifers, while vegetation increase in five springs was attributed to water seepage from agricultural areas upstream. In conclusion, addressing vital habitats such as natural springs in arid drylands requires a holistic approach that integrates long-term climatic, ecological, and anthropogenic observations.

Keywords: drylands; natural springs; aquifers; remote sensing; NDVI

1. Introduction

About 10% of Earth's land area lies within the harsh climatic conditions of the hyper-arid environment (HAE). The HAE is characterized by low rainfall, high evaporation, and extremely high inter-annual variability in rainfall amount and timing [1]. The prevailing climate of the HAE is characterized by long dry phases that are interrupted by extreme, short rainfall events that often generate flash floods. Yearly rainfall in HAEs is less the 5% of the evapotranspiration (aridity index<0.05[2]. Within such extreme aridity conditions, natural springs hold high ecological importance, representing oases of life, boasting remarkable productivity and biodiversity. Springs are recognized globally as biodiversity hotspots [3,4].

Natural springs are sites in which aquifer water discharges aboveground or relatively close to the surface, within reach of vegetation roots. Springs provide water and food resources, as well as vegetated areas, for various animals. They are a known habitat for many endemic fauna and flora species. Springs in arid environments are equivalent to terrestrial islands, and their ecological contribution is often be far beyond their regional context [4–6]. Springs contribute not only to the

 doi:10.20944/preprints202402.0377.v1

natural systems but also to human welfare. By supplying natural resources for agricultural uses, they mitigate harsh climatic conditions [7]. Although their importance has been proven, they often lose the competition between nature conservation and exploitation of natural resources for human benefit. Worldwide, there are numerous examples of natural springs jeopardized by overexploitation of aquifer water [8–11].

The Arava Valley, shared between Israel and Jordan, is located within the HAE. Vegetation in the Arava Valley grows sparsely within ephemeral channels that receive water during flash flooding. Aside from ephemeral channels, vegetation can be found around the natural springs of the Valley. Archaeological evidence near the springs attests their ability to sustain life under harsh climatic conditions. Examples include the chain-well systems of the Early Islamic period [12–14], the Ein Yahav aqueduct and the remains of settlements near the Ein Marzev oasis, related to the Islamic Period [15], and the Bronze Age fort of Ein el-Ghadyan (Ein Yotveta) [16].

A comprehensive study depicting the deterioration of the natural springs of the Arava Valley throughout the late 20th century was published in 2012 (Bruins et al., 2012). The study showed that of the 31 springs found on the Israeli side, 18 of were found to be dry in 2010. The study closely investigated four of these springs based on historical data, and analyzed climatic trends from the 1970s until 2010. They concluded that a mix of climatic and anthropogenic factors caused the springs to dry, namely, decreasing yearly precipitations in the previous decades and over-exploitation of water from the contributing aquifers.

A decade later, our examination of the Israeli Meteorological Survey (IMS) dataset revealed that Bruins et al. (2012) conducted their research during the driest decade recorded in the Arava Valley since rainfall measurements began in the 1950s. Notably, the subsequent decade appears to be one of the wettest in the region's recorded history. Recent reports from the Israeli Water Authority indicate that the yearly water extraction rate from the regional aquifers has not changed significantly since 2000 (Gutman, 2020; 2013).

We hypothesised that the changing regional climatic trend coupled with the relatively consistent water extraction from the aquifers will enable us to differentiate between the effects of climatic conditions and anthropogenic factors on the natural springs of the Arava Valley.

Given that water is the main limiting factor for vegetation cover in the HAE, we assume that monitoring vegetation cover in the vicinity of springs serves as a good indicator for the water supplied by the contributing aquifers. This assumption forms the basis for our research questions:

1. Do changes in the vegetation cover near natural springs in the Arava Valley correspond to the fluctuations in natural rainfall patterns?
2. Can discrepancies between the expected vegetation trends in response to climatic variability be attributed to human activities, such as groundwater extraction or irrigation surplus from agricultural areas?

To answer these questions and achieve a wide spatio-temporal perspective, we integrated time series of remote sensing satellite imagery with climatic records to assess the changes in vegetation cover throughout the entire Arava Valley. We quantified the state of vegetation using the Normalized Difference Vegetation Index (NDVI) [17] and historical imagery, and computed the Standardized Precipitation Index (SPI) to classify climatic sub-periods. The anthropogenic effect was estimated by assessing water extraction from the aquifers and the status of the agricultural plots that are hydrologically connected to the springs.

1.1.1. Our hypotheses:

1. Vegetation cover around the springs corresponds with prevailing rainfall trends;
2. Water extraction from local aquifers decreases the aquifer's water table, negatively impacting the vegetation cover around the natural springs;
3. Surplus water leaching from agricultural plots increases vegetation cover around the natural springs downstream.

2. Methodology

 doi:10.20944/preprints202402.0377.v1

2.1. Study area

The Arava is a long and narrow geographical zone spanning from the southern tip of the Dead Sea to the Gulf of Aqaba (180km long and 5-15km wide). Geomorphologically, the Arava acts as a sedimentary basin bounded by the Negev Highlands to the west and the Jordanian mountains to the east. The Arava ranges in elevation from -380m to 210m above sea level.

The Arava Valley is extremely arid with high values of evapotranspiration. The region is defined as an HAE with an aridity index<0.05 [2,18]. The rainfall in the region originates from two synoptic systems: 1. The Red Sea Trough (RST), carrying precipitation coming from the south, is active mostly during the transitional seasons (October – November and April - May) [19]; 2. The Cyprus lows, carrying precipitation from the Mediterranean Sea generally during the winter season (December - March), mainly affect the northern Arava [20]. Most of the rain events are short and some are intensive; a single event can carry more than 100% of the annual average precipitation. During intensive rain events, runoff generated on the slopes flows down the wadies (ephemeral streams) as flash floods.

2.1.1. Hydrogeology of the Arava Valley

The Arava Valley, a pull-apart basin filled with Neogene to Quaternary sediments, is divided into two primary terminal basins. The central and northern parts of the Valley drain from both sides (east and west) toward the Dead Sea, while southern flows reach either local terminal watersheds (playas) or the Red Sea (Figure 1). However, not all runoff water reaches these terminal base levels. A substantial portion of flash flood water percolates through the soil and recharges the aquifers. The four main aquifers that feed the Arava Valley springs are listed below; their properties are summarized in Table 1.

 doi:10.20944/preprints202402.0377.v1

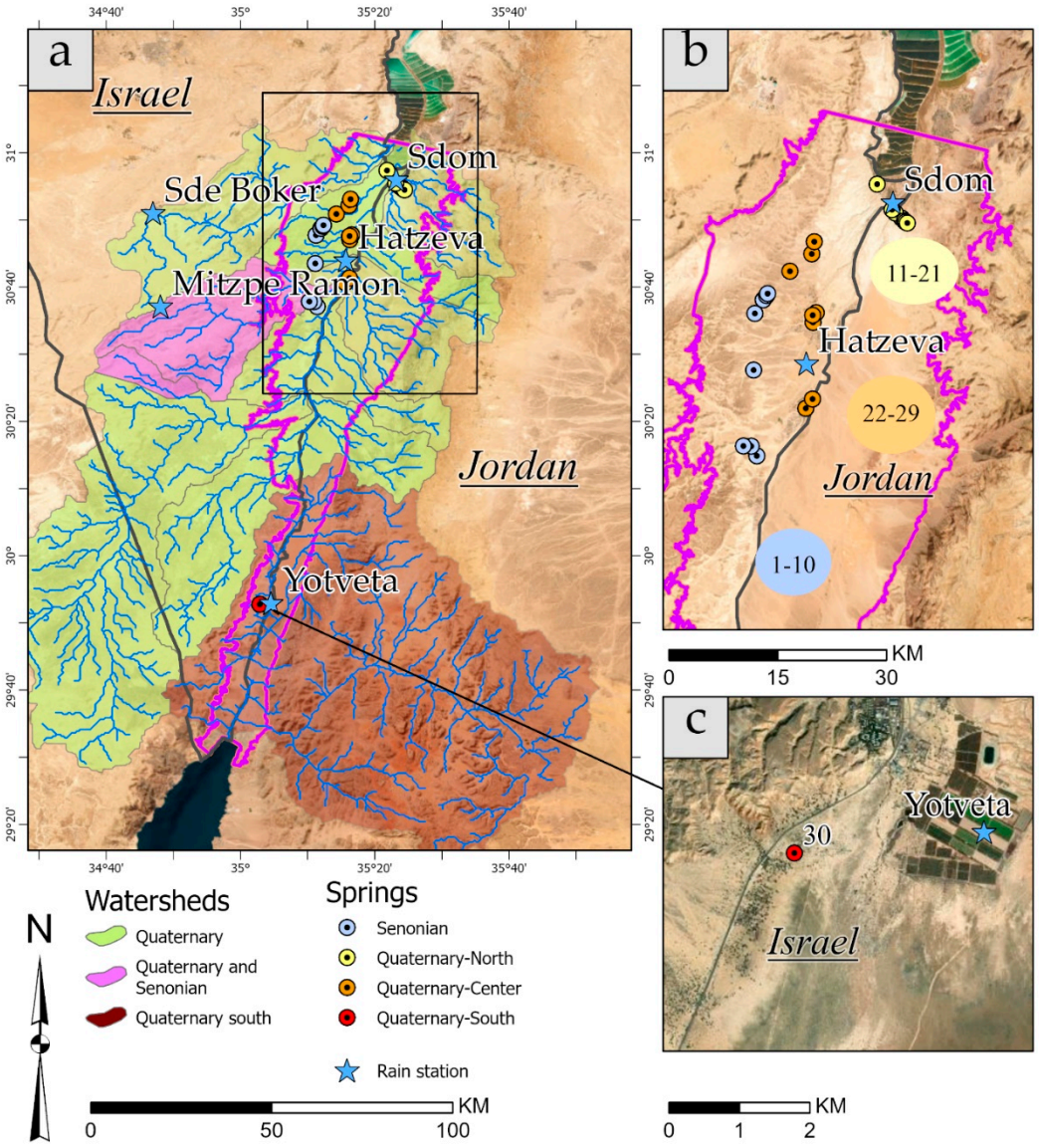

Figure 1. a. A broad overview of the Arava Valley research area (Purple) exhibiting the main watersheds, each associated with the aquifer it can potentially enrich. The Arava springs classified based on their contributing aquifers, and rain stations are marked. b. Inset of the northern Arava; the numbers correspond to the list of springs in Table 1. c. The southernmost spring studied. The background imagery maps are taken from ESRI World Imagery maps, 2023.

1. The Quaternary aquifers are geographically divided into three units: north, center, and south (Qan/Qac/Qas). Due to complex sedimentary interbedding and high hydraulic connectivity, it is reasonable to consider the Neogene aquifer and the Quaternary aquifers as one hydrogeological unit (Guttman et al., 1999). The aquifers recharge from transmission loss during flash floods events from the Negev and the Edom Mountains (Figure 1) [21–23]. The aquifer's thickness is unknown as it varies spatially from hundreds to thousands of meters (Guttman et al., 1999, Yechieli et al., 2001). Springs discharge from these aquifers, emerging at exposed fault lines and formation contacts.
2. The Senonian aquifer (Sa) of the Negev Highlands extends to the west of the Arava Valley; it is fed by two hydrological sources: flash flood transmission losses from the Negev Highlands through the Senonian formation outcrops, and lateral flow from the neighbouring regional aquifers (Burg et al., 2013). The hydrological watershed of the Senonian aquifer overlaps some of the watersheds of the Quaternary aquifers (Figure 1). About 12 springs are related to this

 doi:10.20944/preprints202402.0377.v1

aquifer; they all emerge at the western part of the Arava lowlands, where the aquifer's structure is confined.

Table 1. Overview of the 31 springs identified within the Arava Valley (location shown in Figure 1), including their main hydro-geological context and representative rain station. The asterisk denotes the rain stations used to determine the climatic sub-periods. The threshold column indicates whether the springs qualified to be statistically analyzed according to the study's initial conditions (see Section 3.2.3.2).

#	Spring name	Elevation [m]	Meeting the threshold for analysis	Country	Aquifer	Sub-aquifer	Representative rain stations	Average distance between the cluster of springs and the rain station
1	Ein Zach N	-70	Yes	Israel	Senonian	Mishash	Mitzpe Ramon	~40 km upstream from the springs
2	Ein Zach S	-70	Yes	Israel				
3	Ein Yahav	-24	Yes	Israel				
4	Ein Tamid	-62	Yes	Israel				
5	Ein Mashak	-63	Yes	Israel				
6	Ein Rachel	21	Yes	Israel				
7	Ein Shachak	-55	Yes	Israel			Hatzeva*	~8 km downstream from the springs
8	Ein Moa	39	No	Israel				
9	Shabaya Well	42	No	Israel				
10	Ein Erga	-11	Yes	Israel				
11	Ein Plutit	-370	Yes	Israel	Quaternary North	Lisan	Hatzeva	~25km upstream from the springs
12	Sdom 1	-350	Yes	Jordan				
13	Sdom 2	-350	Yes	Jordan				
14	Sdom 3	-350	Yes	Jordan				
15	Sdom 4	-350	Yes	Jordan				
16	Sdom 5	-350	Yes	Jordan				
17	Sdom 6	-350	Yes	Jordan			Sdom*	~3 km downstream from the springs
18	Sdom 7	-350	Yes	Jordan				
19	Ein Tamar	-370	No	Israel				
20	Fish ponds N	-370	No	Israel				
21	Fish ponds S	-370	No	Israel				
22	Ein Gidron West	-183	Yes	Israel	Quaternary Center	Hatzeva	Sde Boker	~45 upstream from the springs
23	Ein Gidron East	-154	Yes	Israel				
24	Ein Layka	-170	Yes	Israel				
25	Ein Yamluch (Sayf)	-109	Yes	Israel				~12km downstream from the springs
26	Ein Amatzia	-196	Yes	Israel		Samara	Hatzeva*	
27	Ein Ofarim	-176	Yes	Israel				
28	Ein Hufira	-124	Yes	Israel				

 doi:10.20944/preprints202402.0377.v1

29	Ein Marzeva	-121	Yes	Israel				
30	Ein Yotveta	67	Yes	Israel	Quaternary	Samara		~2km downstream
31	Ein Evrona	51	No	Israel	South		Yotveta*	from the springs

2.1.2. Water Dynamics and Human Settlements:

During the first half of the 20th century, the Arava Valley was sparsely populated by Bedouin nomads [25]. Since the establishment of industries west (1936) and east (1956) of the Dead Sea, groundwater exploitation has drastically intensified. The Arava Valley is divided by a political border between Israel (established in 1948) and Jordan (established in 1946). On the Israeli side, water exploitation has expanded to meet the domestic and agricultural demands of its southernmost city, Eilat, established in 1949. Twenty rural settlements were established during the following decades. Currently (2023), the main source of livelihood for the 9,600 rural residents is agriculture, while Eilat (pop. 53,00) remains the single urban settlement. Aqaba is the main city on the Jordanian side of the Arava (pop. ~150,000 in 2015). Its residents are highly dependent on water supply from the Disi aquifer [26]. Four main villages are home to ~10,000 residents (in 2022) who depend on traditional agriculture for their livelihood [27].

2.2. Datasets and preprocessing

This study includes rainfall, meteorological, satellite imagery, hydrological and spatial geographical datasets, and a literature review.

2.2.1. Rainfall dataset

Our rainfall dataset was taken from daily rainfall measurements collected by the Israeli Meteorological Survey (IMS) from each meteorological rain station. Each station has recorded at least 30 years of data and is within the Arava Valley or the contributing upstream watershed[1]. We selected the following meteorological stations that have recorded at least 30 years of rain data: Yotveta (1954-1968, 1974-2022), Hatzeva (1988-2022), Sdom (1959-2022), Mitzpe Ramon (1952-2022), and Sde Boker (1951-2022). Based on the monthly rainfall measurements, we computed the Standardized Precipitation Index (SPI) [28,29] to statistically define the occurrence of wet and dry sub-periods in our study area during the investigated period.

2.2.1.1. Computing the Standardized Precipitation Index (SPI)

The SPI was calculated based on equations given by Kumar et al. and the World Meteorological Organization [30,31]. The data of the long-term monthly rainfall time series from each station was fitted to a gamma distribution function and was thus transformed into a normal distribution. The SPI values can be interpreted as the number of standard deviations by which the observed anomaly deviates from the long-term mean. The SPI values were categorized (Table 2). The SPI was calculated for 36-month windows as advised by the WMO for assessing the effect on reduced reservoir and groundwater recharge. Values were calculated using the Python script given in a GitHub page [32].

2.2.1.2. Relating the rain stations to springs

Each cluster of springs was associated with its closest rain station, provided that the rain station was situated within the same watershed basin as the cluster of springs (Figure 1). We surveyed the geological setting of the watershed to determine whether it had the potential to recharge the aquifer

[1] Though the Arava Valley receives water also from the Jordanian side, we do not have access to this data, thus we had to ignore its possible contribution.

 doi:10.20944/preprints202402.0377.v1

associated with the cluster of springs. The spring clusters, associated rain stations, and their properties are detailed in Figure 1 and in Table 1.

2.2.2. Identifying the springs' location and vegetation coverage:

The springs on the Israeli side were mapped using the Open Landscape Institute (OLI) surveys [33]. Several springs in the Jordanian Arava were identified using 1980 Israeli Defence Force 1:50,000 topographical maps (Figure S1), which feature the physical geography of Jordan. Each spring's location was transformed into a GIS polygonal entity based on the vegetation cover surrounding the spring. The vegetation cover was marked, and the area was assessed twice, using Corona satellite imagery and Planet satellite images, as follows:

- We used historical Corona satellite imagery (3 m) taken on 7/05/1968 [34] to delineate the area of spring-dependent vegetation around each spring. Although the Corona satellite used a panchromatic sensor, the high contrast in the albedo between the bright soil and the vegetation cover of springs in the desert environment creates a distinguishable feature that can be mapped [35] (Figure 2a, c). The imagery was taken before water was extracted from Arava aquifers, thus the conditions are considered to have been relatively natural.
- We evaluated the extent of vegetation cover in May 2022 (late spring), using the NDVI images calculated from Planet satellites (3 m resolution) [36] (Figure 2b, d). Comparing between the recent and historical imagery can reveal the anthropogenic effect on the local water cycle as reflected by changes in vegetation cover.
- Additionally, we incorporated data on the extent of vegetation cover surrounding each spring during 2009-10, as reported by Bruins et al. (2012).

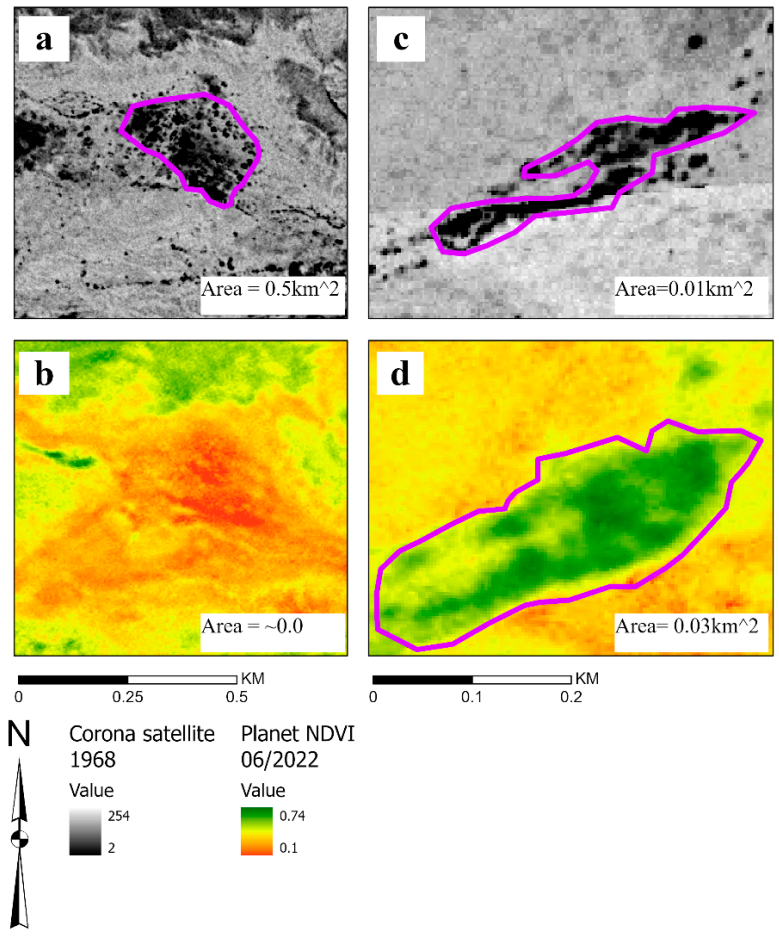

Figure 2. Evaluating the change in extent of vegetation cover near two springs by comparing Corona historical satellite imagery taken in 1968 with Planet imagery taken in 2022. a. Ein Rachel (7.05.1968), b. Ein Rachel (26.06.2022), c. Ein Gidron east (7.05.1968), d. Ein Gidron east (26.06.2022).

 doi:10.20944/preprints202402.0377.v1

2.2.3. Estimating yearly perennial vegetation activity

To quantify the changes in the state of perennial vegetation over the last four decades, we used NDVI computed from Landsat Level 2, Collection 2, Tier 1 product [38,39]. We created a continuous database imagery from 1984 to 2022, using Landsat 5, 7, and 8 satellite images. Data from 2011 was not used because of a Landsat 7 satellite malfunction [40]. The images from the sequence of satellites were harmonized, atmospherically corrected, and downloaded at a spatial resolution of 30 m using the Google Earth Engine (GEE) Platform.

To derive the perennial vegetation proxy from the NDVI data, we followed the typical phenological cycle of the perennial vegetation in the Arava Valley. Perennial vegetation is photosynthetically active throughout the year but shows its highest spectral response in early summer [41,42]. Thus, for each yearly imagery sequence of the Landsat time series, we took the maximum NDVI values at each pixel, which were found between May and June. This time series is referred to as $NDVI\ max_{May-June}$.

Using the $NDVI\ max_{May-June}$ time series, we estimated yearly changes in perennial vegetation within the polygons which were created according to the vegetation cover in 1968. As the $NDVI\ max_{May-June}$ time-series starts in 1984, we calculated yearly changes in perennial vegetation between 1984 and 2022.

2.2.3.1. Spring vegetation activity time series grouped according to aquifer

We grouped the results based on the main contributing aquifer of each cluster of springs, based on the hydro-geological background given in Section 3.1.1.

We used Spearman's correlation test to compute the correlation matrix between the vegetation of the different springs, throughout the time series of annual $NDVI\ max_{May-June}$ within each group of springs. The complete matrices are provided in Tables S1-S3. The average (Av.), median (M.), and the standard deviation (Std.) values are detailed in Section 4 (Results). In cases for which the average correlation between the vegetation around the springs within an aquifer was >0.8, we merged the results and plotted the average, lower, and upper quartiles of the NDVI time series.

2.2.3.2. Threshold for analysis of the vegetation cover

As the study is based on remote sensing and not on field sampling methods, we defined two conditions as threshold limits to determine which springs should be included in our time series analysis. The thresholds ensure that the springs' vegetation is natural and that it can be detected using remote sensing methods.

a. Land use mapping: We excluded springs whose current land use definition was not defined as "natural" according to ESRI 2020 land use maps *(https://livingatlas.arcgis.com/landcover/)* (i.e., built up and agricultural areas).
b. NDVI threshold: Given our limited ability to identify vegetation around the spring, we set a threshold limit of NDVI > 0.2 using the first three years of the Landsat time series (1984-1987). Our spatial analysis indicated that natural vegetation within ephemeral channels during May and June does not exceed an NDVI of 0.2. Therefore, pixels with NDVI values higher than this threshold are most likely supported by underground water sources. We chose the first three years of the time series, as they reflect natural vegetation conditions.

- Altogether we mapped 31 springs; 25 of them met both of our requirements and were statistically analyzed.

2.2.4. Aquifer water extraction data set

Data on yearly water extraction from each aquifer was obtained from the Israel Hydrological Service database.

2.3. Data analysis

 doi:10.20944/preprints202402.0377.v1

We assessed changes in the vegetation cover of the natural springs in the Arava Valley as a function of climatic and anthropogenic conditions using the methodological approach detailed below (Figure 3).

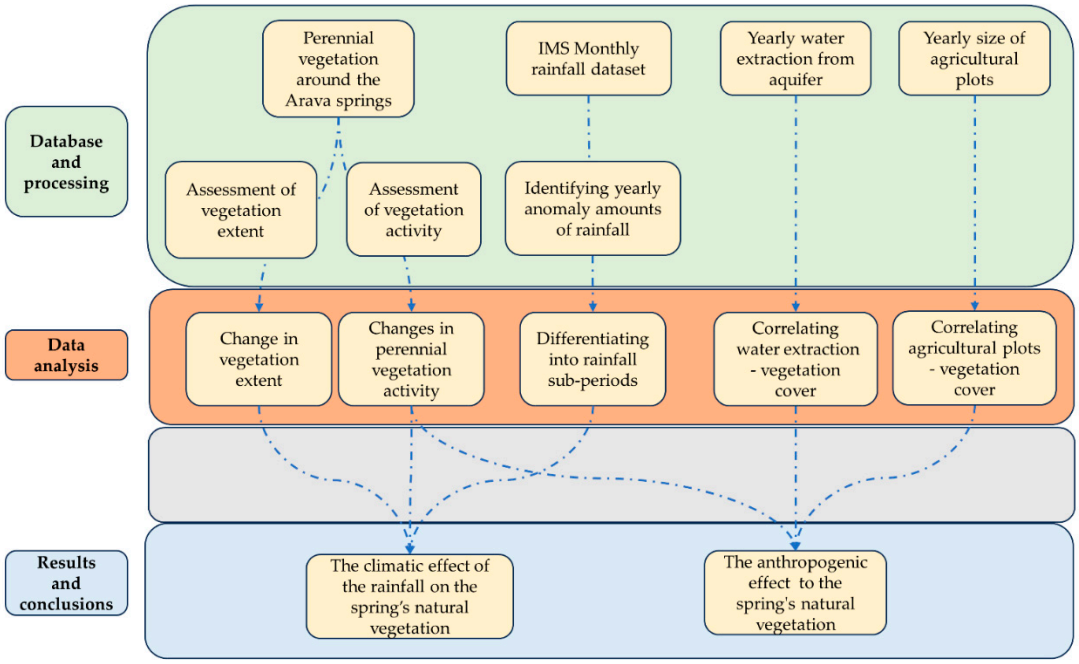

Figure 3. The figure illustrates the methodological approach used in this research. The vegetation was assessed at three time periods: 1968 (Corona satellite), 2009-10 (Bruins et al. 2012), and May 2022 (Planet satellite). Vegetation cover was assessed with the $NDVI\ max_{May-June}$ time series. Yearly rainfall anomalies were identified by calculating the SPI in 36-month windows.

2.3.1. Identifying wet and dry sub-periods

We identified wet and dry sub-periods using the 36-month SPI computation, to study the cumulative impact of consecutive wet/dry years on vegetation cover near the springs. A sub-period was considered wet for months in which the maximum SPI value within a moving window of 19 months was ≥ 1, and dry for months in which the minimum SPI value within a moving window of 19 months was ≤ -1. A period of 19 months was chosen as it is about half of the 36-month period used for the SPI calculation (+1 to evenly account for periods before and after each assessed year).

Table 2. The classification of SPI values based on McKee et al. (1993) and Svoboda et al. (2012).

SPI values	Drought and humid category
≥ (+) 2	Extremely wet
(+) 1.5 to (+) 1.99	Very wet
(+) 1 to (+) 1.49	Moderate wet
0 to (+) 0.99	Mild wet
0 to (-) 0.99	Mild drought
(-) 1 to (-) 1.49	Moderate drought
(-) 1.5 to (-) 1.99	Severe drought
≤ (-) 2	Extreme drought

2.3.2. Evaluating the response of the spring vegetation to the wet and dry sub-periods

 doi:10.20944/preprints202402.0377.v1

We used the closest meteorological station to define the effect of wet and dry sub-periods on the vegetation of each spring cluster. Meteorological stations which are farther upstream but share the same watershed were added to achieve the maximum potential data of rainfall affecting each cluster of springs. These stations were analyzed in case discrepancies between the rainfall station and the vegetation cover were identified. The list of aquifers and their related meteorological stations is given in Table 1.

We identified statistically significant differences in the average NDVI values of the $Landsat\ NDVI\ max_{May-June}$ between each sub-period transition (wet to dry and vice versa) using the Mann-Whitney U test (i.e., U test for non-normal distributions) at $p < 0.05$. A positive significant shift in the NDVI values indicated an increase in the perennial vegetation activity, and a negative shift indicated a decline. Additionally, we examined the trend in $Landsat\ NDVI\ max_{May-June}$ throughout the entire period using the Mann-Kendall Tau test [43]; $p < 0.05$ was considered significant.

2.3.3. Evaluating the anthropogenic effect on the springs' perennial vegetation

We assessed the potential impact of two anthropogenic factors, water extraction and agriculture, that may affect the perennial vegetation around the springs. The correlation between these factors and perennial vegetation was estimated as follows:

2.3.3.1. Water extraction from each aquifer (per year):

- Correlations between annual water extraction from the aquifers and the yearly values of the $Landsat\ NDVI\ max_{May-June}$ cover around the springs were evaluated using Spearman's correlation test. We considered p-values below 0.05 to be statistically significant.
- We assumed that water extraction from the aquifer negatively impacts vegetation cover. Positive correlations, indicating that increased water extraction led to increased vegetation cover, were disregarded, as they likely represent statistical artefacts.

2.3.3.2. Effect of the agricultural plots upstream of the springs

We assessed the size properties of the agricultural plots located upstream from springs, as a potential source of water that reaches the springs. The analysis was conducted as follows:

- We calculated the distance between each spring to the closest agricultural field using the ESRI 2020 land use map [44].
- We assumed that the springs that benefit from irrigation seepage share a hydrological connection with the plot. A spring that is downstream of an agricultural plot, not farther than 20 km, was considered to be connected to the plot. Springs that did not meet this criterion were omitted.
- To estimate the annual area of cultivated plots, we generated a time series using the yearly minimum of the NDVI from Landsat imagery (similar to the production of the perennial vegetation time series) and created a yearly mosaic of the minimum NDVI values, i.e. $Landsat\ NDVI_{min}$.
- At the end of the summer, the NDVI values of the natural vegetation are very low, whereas irrigated areas maintain significantly higher NDVI values, enabling to distinguish between natural and irrigated vegetation.
- We set a threshold limit of $Landsat\ NDVI_{min} > 0.2$, to differentiate between irrigated and non-irrigated areas, and calculated the size of agricultural areas (pixels exceeding this threshold).
- We used Spearman's correlation test (at $p<0.05$) to assess the relationship between the $Landsat\ NDVI\ max_{May-June}$ values of the springs throughout the time series and the size of each agricultural area, for each year.

3. Results

3.1. Wet and dry sub-periods in the Arava Valley

 doi:10.20944/preprints202402.0377.v1

Data from the two meteorological stations in the southern–central part of the Arava Valley (Yotveta, Hatzeva) documented a wet period (1985/1987-1997/1993), followed by a dry period (2003/1998-2014) and then another wet period (from 2015 onwards) (Figure 4, Table 3). The Sdom station in the northern Arava experienced two consecutive dry phases (1978-1986, 1997-2004) followed by two consecutive wet periods (2005-2013, 2015-2021). The Sde Boker station experienced two wet sub-periods (1980-1984, 1986-1995) followed by several dry sub-periods since 1997. The Mitzpe Ramon station recorded fluctuating yearly precipitation, without any wet or dry sub-periods.

Table 3. Wet and dry sub-periods were identified based on the 36-month SPI calculation of data from each station (Figure 4). We evaluated the response of perennial vegetation around each spring to sub-period transitions.

Rain station	Rainfall sub-periods; 1980 -2022		
Yotveta	Wet 1985-1997	Dry 2003-2014	Wet 2015-2023
Hatzeva	Wet 1987-1993	Dry 1998-2005, 2008-2014	Wet 2015-2022
Sdom	Dry 1978-1986	Dry 1997-2004	Wet 2005-2013, 2015-2021
Sde Boker	Wet 1980-1984 1986-1995	Dry 1998-2007, 2010-2015, 2017-2020, 2021-2022	
Mitzpe Ramon	None identified		

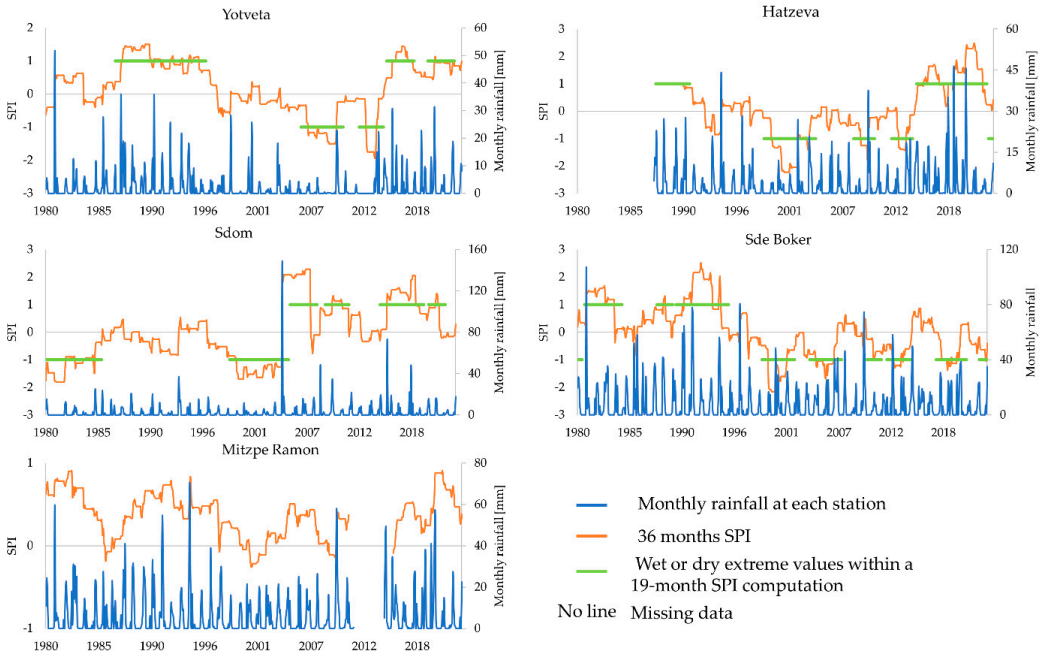

Figure 4. Monthly rainfall measurements recorded at the five meteorological stations of the Arava Valley (blue) and calculated SPI based on a 36-month window (orange). The horizontal green lines represent clusters of months in which the maximum (> 1) or minimum (< -1) value within a moving window of 19 months was defined as wet or dry (see Section 3.3.1). Table 3 depicts the climatic sub period for each station.

 doi:10.20944/preprints202402.0377.v1

3.2. Vegetation cover trends around the natural springs:

3.2.1. Springs of the Senonian aquifer

The time series of the vegetation cover of the Senonian aquifer springs over the last four decades is presented in Figure 5a. The correlations between the yearly vegetation cover around each of the springs along the time series are low (corr. av.= 0.45, m.=0.32, Std.=0.32), indicating the great variability along the time series within the Senonain springs. The perennial vegetation surrounding the springs is subjected to fluctuating rainfall as recorded by the Hatzeva and Mitzpe Ramon stations. The Hatzeva stations experienced a transitions from wet - dry - wet sub-periods, while the Mitzpe Ramon stations hasn't recorded any recognizable sub periods (Table 3). The perennial vegetation cover surrounding six of the eight Senonian springs declined significantly ($p < 0.05$) following the transition from the wet to dry sub-period. Five of the springs recovered significantly ($p < 0.05$) during the third (wet) sub-period. Observing the entire inspected period (Table 4 Mann-Kendall Trend; 1984-2022) illustrates the statistically significant negative trend of six springs. We identified a decrease in the vegetation cover in all of the Senonian springs between 1968 and 2022 (Table 4). In three of the eight springs, cover decrease was so significant that the vegetation could not be identified in the 2022 imagery (e.g., Ein Rachel; Figure 2a vs 2b). Several field images demonstrating the typical vegetation in selected springs are presented in Figure 6. Ein Yahav (#3) is an example of a spring with high vegetation mortality; a cluster of dead reeds and spiny rush (*Phragmites australis* and *Junus Acutus*) is shown (Figure 6a). Ein Tamid (#4) is an example of a spring in which the vegetation cover hasn't declined during the last decade (Figure 6b). Figure 6c shows a photo of Ein Shachak (#7) in 2012, while Figure 6d was taken at the same place in 2022. The two images demonstrate the extreme decline in the vitality of the spring's vegetation after one decade. The yearly extraction rate of the Senonian Aquifer was very low during the early 1980s, increased significantly since 2009. Currently, about 2 MCM of water are extracted annually.

Table 4. Vegetation parameters of the springs which met the study's threshold limits. The results include the estimated vegetation cover area around each of springs at three time periods, and the precent of cover area increase or decrease comparing between the second and first estimations (C1%), and between the third and the first estimations (C2%). Additionally, the response of the perennial vegetation around the springs to each climatic shift, based on the SPI calculation and the overall trend between 1984 – 2022 ($Mann\ Kendall_{sig \leq 0.05}$.).

#	Spring name	Aquifer	Sub aquifer	Estimated vegetation cover [m^2] around each spring					Perennial vegetation response to climatic shifts, based on yearly maximum NDVI values in May - June from Landsat time series		
				1968	2009-2010	2022	C1%	C2%	Shift 1 (wet to dry)	Shift 2 (dry to wet)	Mann-Kendall Trend (1984-2022)
1	Ein Zach N	Senonian	Mishash	13,000	7,500	7,100	58	55	↘	→	↓
2	Ein Zach S			5,100	No data	3,400	?	67	↘	↗	→
3	Ein Yahav			15,000	44,200	3,200	295	21	↘	→	↓
4	Ein Tamid			22,100	13,500	10,000	61	45	↘	↗	→

 doi:10.20944/preprints202402.0377.v1

5	Ein Mashak			8,900	4,750	X	53	~0	↘	↗	↓
6	Ein Rachel			52,200	48,000	X	92	~0	↘	→	↓
7	Ein Shachak			3,750	1,400	770	37	21	↘	→	↓
10	Ein Erga			10,400	4,280	X	41	~0	↘	→	↓
11	Ein Plutit	Quaternary North	Lisan	29,000	25,300	28,000	87	97		↗	↑
12	Sdom 1			5,700	No data	50,000	?	877		↗	↑
13	Sdom 2			2,000	No data	10,000	?	500		↗	↑
14	Sdom 3			800	No data	2,400	?	300		↗	↑
15	Sdom 4			780	No data	2,800	?	359		↗	↑
16	Sdom 5			10,900	No data	20,000	?	183		↗	↑
17	Sdom 6			10,300	No data	25,000	?	243		↗	↑
18	Sdom 7			9,500	No data	20,000	?	211		↗	↑
22	Ein Gidron West	Quaternary Center	Hatzeva	18,300	18,800	25,000	103	137	↘	↗	→
23	Ein Gidron East			11,700	30,480	26,200	261	224	→	↗	↑
24	Ein Layka			7,210	No data	15,340	?	213	→	↗	↑
25	Ein Yamluch (Sayf)			39,880	9,000	10,060	23	25	↘	↗	↓
26	Ein Amatzia		Samara	5,600	5,630	9,840	101	176	→	↗	↑
27	Ein Ofarim			50,000	34,000	74,500	68	149	→	↗	↑
28	Ein Hufira			39,030	15,000	43,000	38	110	↘	↗	↑
29	Ein Marzeva			4,000	6,000	60,000	150	1500	→	↗	↑
30	Ein Yotveta	Quaternary South	Samara	60,000	64,750	70,000	108	117	↘	↗	→

 doi:10.20944/preprints202402.0377.v1

C1/C2	If the change in the cover area) was larger (green) or smaller (red) than 10% of the area in 1968
↗↘	Statistically significant (based on Mann Whitney u test, $p \leq 0.05$) positive (green) or negative (red) shift in the vegetation cover between the climatic periods,
↑↓	Statistically significant (based on Mann Kendall Tau, $p \leq 0.05$) positive (green) or negative (red) trend for the entire inspected period,
→	No statistical shift or trend was identified in the vegetation cover.
x	The vegetation cover became too sparse and could not be identified.
No data	The springs were not studied by Bruins et al. (2012)

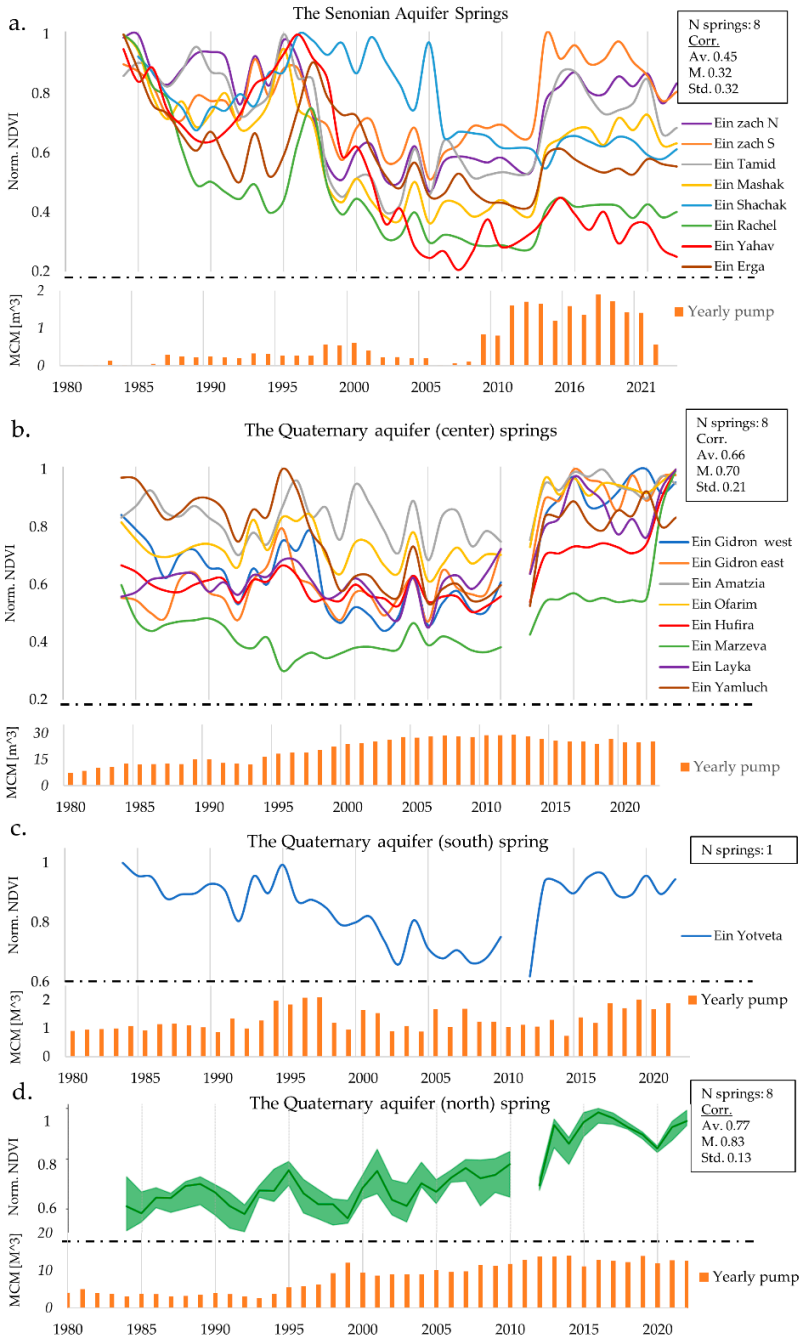

 doi:10.20944/preprints202402.0377.v1

Figure 5. NDVI values around each of the natural springs and the annual water extraction from each aquifer. The NDVI values shown here were normalized relative to maximum annual value of each spring, for ease of comparison. The statistical analysis results, as presented in Table 4, are based on the data provided here. The black box at the right side of each graph summarizes the correlation among the springs associated to each aquifer.

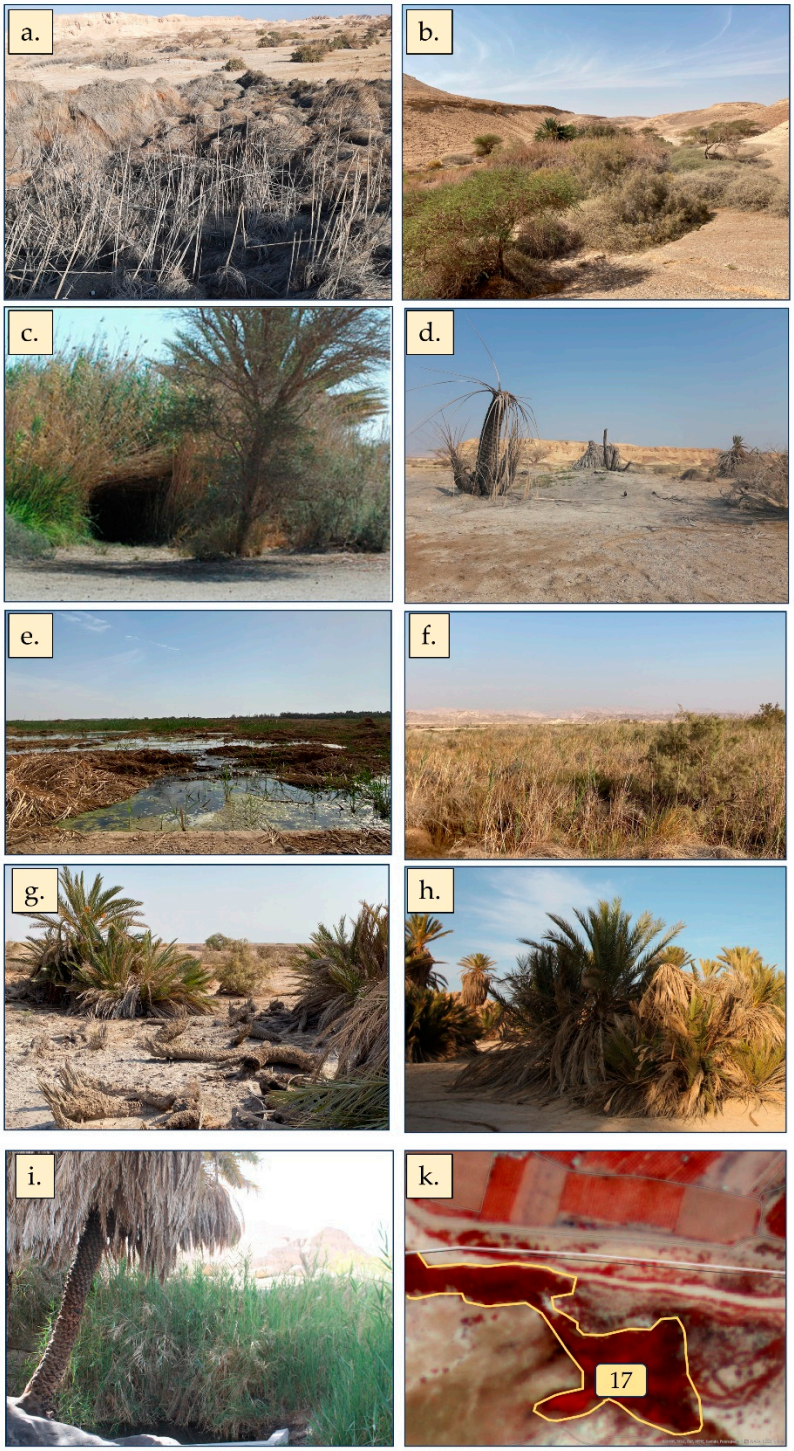

Figure 6. Selected images of springs in the Arava Valley. The aquifers and date taken are indicated in the parentheses. All images, apart from 6c and 6k, were taken by Ariel Meroz. a. Ein Yahav (SA) (30/12/2022), b. Ein Tamid (SA) (19/10/2023), c. Ein Shahak (SA) (2012), photo by Roy Galili, d. Ein Shahak, (SA) (30/12/2022), e. Ein Hufira (QAC) (19/10/2023), f. Ein Ofarim (QAC), (19/10/2023) g. Ein Yamluch (QAC) (19/10/2023), h. Ein Yotveta (QAS) (19/10/2023), i. Ein Plutit (QAN) (19/10/2023), k.

 doi:10.20944/preprints202402.0377.v1

Spring # 17 (QAN), Planet NDVI imagery (26/06/2022) the red color emphasizes the dense vegetation around the spring.

3.2.1.1. Correlation between the yearly water extraction and the vegetation cover

We found that vegetation cover of four of the eight Senonian springs correlated negatively with the amount of water being extracted from the aquifer (quantified by the $Landsat\ NDVI\ max_{May-June}$). The springs affected by water extraction are up to ~6 km from the well (Table 5).

3.2.2. Springs of the Quaternary aquifer (center):

The yearly vegetation cover among springs of the Quaternary aquifer (center) have correlated moderately well during the past four decades (Figure 5b; corr. av.= 0.66, m=0.7, Std=0.21). The perennial vegetation surrounding the springs is mostly subjected to rainfall transitions as recorded by the Hatzeva station; the SPI calculation indicates three sub-periods: wet – dry – wet (Table 3). The perennial vegetation cover of three of the aquifer's eight springs declined significantly ($p<0.05$) following the transition from the first (wet) to second (dry) sub-period (Table 4). However, all eight springs demonstrated a statistically significant positive trend following the second shift (from dry to wet sub-period). When analyzing the NDVI of the entire period (Table 4; Mann-Kendall Trend; 1984-2022), six springs exhibit a statistically significant positive trend. In one spring (#25), NDVI significantly declined, and one spring (#22) has no consistent trend. Between 1968 and 2022 (Table 4), the vegetation cover extent increased in two springs and decreased in three following the transition from wet to dry, after the second transition (to wet), six of the eight springs recovered. These results coincide with the overall NDVI trends.

Ein Yamluch (#25) is the only Quaternary aquifer (center) spring whose vegetation showed a significant negative correlation with water extraction from the aquifer (Table 5, corr.= -0.63). Note that topographically, Ein Yamluch is the highest Quaternary aquifer (center) spring.

Water extraction from the aquifer commenced in the 1970s (prior to the period covered by the graph) and steadily increased over time, reaching a peak of approximately 30 MCM/y in 2012, and has fluctuated since. Notably, the volume of water extracted from the Quaternary aquifers is much greater than from the Senonian aquifer.

3.2.2.1. Correlation between the agricultural area and the perennial vegetation cover

Out of the 46 springs that were mapped and statistically analyzed in the Arava Valley, five may have a potential hydrological input from agricultural areas (Figure 7). Notably, all five are Quaternary aquifer (center) springs. The results presented in Table 6 illustrate the extent of correlation, as determined through Spearman's test with a significance level of $p<0.05$, between each spring and the corresponding agricultural area, between 1984 - 2022.

The thriving green reeds and tamarix trees (*Phragmites australis* and *Tamarix*) are evidence for constant water flow in Ein Hufira (Figure 6e). Figure 7 and Table 6 indicate that Ein Hufira likely benefits from agricultural surplus. The high vegetation cover of green reeds and tamarix trees around Ein Ofarim (Figure 6f) is compatible with the high NDVI values in the last decade. Progressive mortality of the date palm (*Phoenix dactylifera*) is evident in Ein Yamluch (Figure 6g).

Table 5. Correlation between perennial vegetation cover around the springs and yearly water extraction rates from both the Senonian and Quaternary aquifers; 1984-2022. Only one spring significantly correlated with the Quaternary aquifer, thus, others are not presented in the table. The asterisk denotes a significance level of $p < 0.05$.

#	Spring name	Aquifer	Distance to the closest well (km)	Level of correlation
1	Ein Zach N	Senonian aquifer	16.0	0.04
2	Ein Zach S		15.8	0.50*

 doi:10.20944/preprints202402.0377.v1

4	Ein Tamid		15.3	0.03
5	Ein Mashak		13.5	-0.05
7	Ein Shachak		6.3	-0.47*
6	Ein Rachel		0.17	-0.43*
3	Ein Yahav		0.3	-0.56*
10	Ein Erga		0.9	-0.41*
25	Ein Yamluch	Quaternary aquifer (Center)	4.8	-0.63*

Table 6. Spearman's correlation (1984-2022) between the yearly maximum NDVI value ($NDVI\ max_{May-June}$) and the size of agricultural plots with potential hydrological connection. Only the springs identified as potentially being hydrologically connected to agricultural plots are presented. The asterisk denotes a significance level of $p<0.05$.

#	Spring name	Aquifer	Distance to upstream agricultural area (m)	Year agricultural area was first established	Level of correlation
23	Ein Gidron east	Quaternary aquifer (Center)	200	2012	0.79*
22	Ein Gidron west		350	2012	0.78*
24	Ein Layka		300	2012	0.85*
28	Ein Hufira		10	Before 1968	0.62*
29	Ein Marzeva		10	Before 1968	0.81*

Preprints.org (www.preprints.org) | NOT PEER-REVIEWED | Posted: 6 February 2024 doi:10.20944/preprints202402.0377.v1

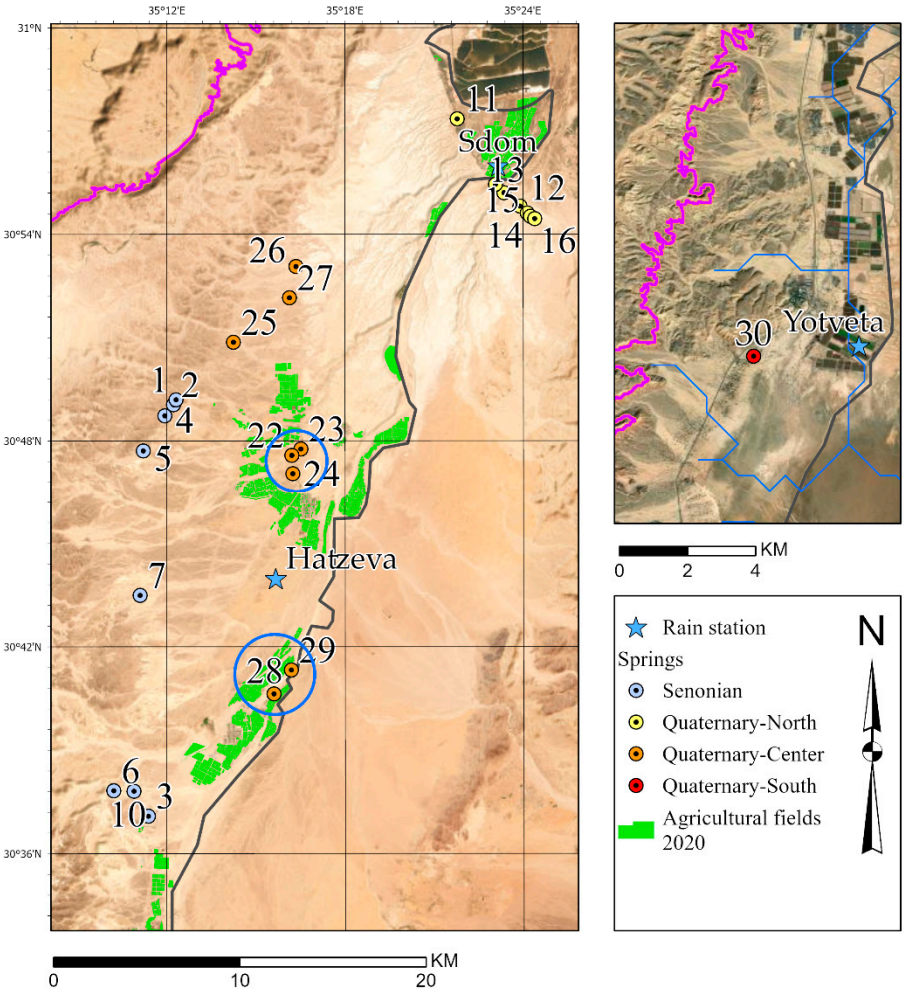

Figure 7. The blue circles encompass the springs that may be influenced by irrigation water leaching from agricultural plots upstream, based on ESRI 2020 LULC maps (Venter et al., 2022). The background imagery maps are taken from ESRI World Imagery maps, 2023.

3.2.3. The Quaternary aquifer (south):

Ein Yotveta is the only spring fed by the Quaternary aquifer (south). Based on the SPI calculated using data from the Yotveta station (Table 3), the perennial vegetation surrounding the springs experienced two climatic transitions: wet - dry - wet sub-periods (Figure 4c). The perennial vegetation cover in Ein Yotveta declined following the first transition and recovered during the second wet sub-period (Table 4). Overall, no significant trend during the last four decades was identified. We identified a minor expansion in the vegetation cover around Ein Yotveta following the second transition. Dense vegetation (mainly date palms) characterizes the spring (Figure 6h). Water has been extracted from the aquifer since the mid-70s (before the period presented in the graph) at relatively low volumes. From the 1980s until 1995, about 1 MCM/y was extracted, and since then, water extraction has increased and currently fluctuates between ~1.5 to 2 MCM/y [45].

3.2.4. Springs of the Quaternary aquifer (north):

The time series of the vegetation of Quaternary aquifer (north) springs in the last four decades is presented in Figure 5d. The internal correlation matrix of vegetation cover among these springs reveals high levels of correlation (corr. av.= 0.77, m.=0.83, Std.=0.13). The perennial vegetation surrounding the springs is mostly subjected to rainfall transitions as recorded by the Sdom station. The SPI calculated from the Sdom station data (Table 3) indicates one significant transition from dry to wet conditions around 2004-5. The vegetation of most of the eight springs related to this aquifer has increased substantially (Table 4); in one case (#12), the vegetated area increased by almost one

 doi:10.20944/preprints202402.0377.v1

order of magnitude compared to the area identified in 1968. Accordingly, the Mann-Kendall trend analysis of all eight springs has shown a significant increase in the perennial vegetation cover. Figure 6i shows the high vegetation cover of reeds and a date palm, and the overflowing water in Ein Plutit (#11). The majority of the springs of this aquifer are in Jordan, and could not be photographed by us. A high-resolution image (3m/pic.) taken from the Planet Inc. satellite emphasizes the dense vegetation of Spring #17 (Figure 6k). Water extraction from the aquifer began in the 1950s (before the period presented in the graph) and was relatively steady at 3-5 MCM/year. Since 1997, extraction rates have increased and currently fluctuate between 8-14 MCM/y (Figure 5d).

4. Discussion

The natural springs of the Arava Valley, situated within the hyper-arid environment (HAE), were used as a unique case study to distinguish between the effects of human activities and climate on the vegetation cover around springs. In this study, we integrated spatial climatic data with vegetation cover and photosynthetic activity derived from satellite imagery, along with records of aquifer water extraction and land use changes. This approach enabled us to assess the resilience of the aquifers to support a stable ecological habitat under natural climatic fluctuations and a growing demand for natural resources.

4.1.1. Identifying climatic sub-periods in the Arava Valley

In this study, we identified wet and dry sub-periods in the Arava Valley based on a 36-month SPI calculation combined with the assessment of defined extreme SPI values. [46] studied the impact of extremely wet or dry years on the flow discharge of karst aquifer springs in the Judean Mountains, using ±1σ (standard deviation) of the multi-year precipitation index to define wet and dry years, based on the method described by[47]. Our approach enabled us to evaluate changes in vegetation without considering the time lag effect of recovery or decline of dryland vegetation [48,49]. In addition, the 36-month SPI calculation made it possible to account for groundwater table changes (WMO, 2013).

Of the five meteorological stations in our area, we found high responsiveness of the vegetation to rainfall data collected from the three Arava Valley stations: Yotveta, Hatzeva, and Sdom. Data collected from the upstream stations (Mitzpe Ramon and Sde Boker) did not correlate well with the vegetation cover, thus were omitted from further analyses. Yotveta and Hatzeva stations exhibited similar climatic sub-periods (wet-dry-wet), whereas the Sdom station recorded only one transition from two consecutive dry periods to a wet sub-period around 2004-5. We attribute this difference to the main synoptic weather systems bringing rain to each station. Yotveta and Hatzeva, the southern stations, are mostly influenced by the Red Sea Trough , whereas the Sdom station, at the northern tip of the Arava Valley, receives rain from the Cyprus lows [19,50,51].

4.1.2. The response of the springs' vegetation to the climatic sub-periods

Using the satellite-derived NDVI time series, we estimated the extent of vegetation around 25 natural springs in the Arava Valley. Our findings revealed that over the past four decades, vegetation cover in fourteen of these springs increased, decreased in seven, and showed no statistically significant change in four. Notably, six of the seven springs that experienced a decline were associated with the Senonian aquifer, and one spring was related to the Quaternary (center) aquifer. The study by [21] indicated that as of 2010, 18 of the 29 studied springs were in a drying phase, according to vegetation cover and water flow.

Twenty one of the springs studied in the current researched were also assessed by [21]. The first climatic transition we identified (2014) was very close to the study by Bruins et al. (2012). Our results, presenting a significant decline in the vegetation of 13 springs of the 21 shared springs at that time, accord with the results of Bruins et al., 2012.

 doi:10.20944/preprints202402.0377.v1

4.1.2.1. Response of vegetation cover to the prevailing rainfall conditions and the anthropogenic factors

Following the initial shift from wet to dry sub-period, the vegetation cover of springs fed by the Senonian aquifer aligned with our initial assumption, displaying a statistically significant decline in all of the springs. Accordingly, we anticipated that the second shift, from dry to wet, would lead to a notable increase in vegetation cover. However, our analysis revealed an increase only in three out of the eight springs; overall the vegetation cover declined throughout the entire period. We attribute this negative trend to anthropogenic activity as the prevailing climatic conditions should have supported an increase in vegetation. Since 2009, water extraction from the Senonian aquifer has increased substantially (Figure 4a); the current extraction rate is approximately 1.5-2 million cubic meters per year. The increasing extraction rates have presumably lowered the water table, consequently limiting the availability of water for vegetation to respond to the improved climatic conditions. As evident in Figure 1 and Table 5, the springs in which vegetation cover has decreased the most are the ones that are the closest to the wells from which water is extracted: Ein Rachel, Ein Erga, and Ein Yahav. Unfortunately, the 1968 maps (Table 4) show that at the time, these Senonian aquifer springs were largest in vegetation cover.

A conversation with residents of the region revealed additional information regarding anthropogenic effects on the natural springs. According to a resident of Ein Yahav, a settlement near Ein Yahav spring (Amnon Navon; private communication 30/12/2022), part of the aquiclude was damaged by infrastructure construction while establishing the settlement in the 1960s (Mishash dome; [52]). This damage causes large volumes of water to drain directly out of the aquifer, permanently affecting the capacity of the aquifer to recharge to its original water table level, and directly affecting the spring. According to the $NDVI\ max_{May-June}$ time series, the perennial vegetation flourished during 1980s, but collapsed during the dry sub-period (1997-2014), and has not recovered since, even after the transition to a wet period. Of the eight springs associated with the Quaternary (center) aquifer, four experienced a significant decline during the first climatic shift from wet to dry. However, most of the springs exhibited a positive trend during the second climatic shift. Consequently, vegetation cover has increased in most of these springs from 1984 to 2022. Although water extraction from the Quaternary aquifer was more than an order of magnitude greater than from the Senonian aquifer, the vegetation cover around the Quaternary springs seems to be less influenced by the water extraction, and its springs recovered during the wet sub-period. This could be explained by the different hydrogeological setting of the two aquifers, mainly their size and the size of the contributing watershed. An exceptional case is Ein Yamluch (of the QAc) where vegetation declined in area and photosynthetic activity. As shown in Table 4, Ein Yamluch is situated topographically higher than the other Quaternary springs. Therefore, it is reasonable to assume that it will be the first to be impacted by local groundwater depletion. This observation may serve as a predictive indicator in case of drought or increased water extraction.

In five instances (Table 6 and Figure 7) we found a strong positive correlation between the size of agricultural plots located upstream of springs and vegetation cover around the springs, which benefit from water seepage from those agricultural areas. This high correlation may obscure the true effect of water extraction on groundwater levels in the vicinity of each spring. This result coincides with previous studies [45,53,54], that found contaminants from agricultural sources in the Quaternary (center) aquifer.

According to our statistical analysis, the vegetation cover around the northern Quaternary aquifer springs increased in cover area and photosynthetic activity. The Israeli hydrological report for the area [55] claims that the aquifer's water level has dropped negligibly in the recent years, but has also identified an increase in nitrate concentrations, from agriculture, which may increase the natural vegetation productivity.

Vegetation surrounding the Ein Yotveta spring, which is feeds from the southern Quaternary aquifer, seems to coincide with the climatic sub-periods which we identified, as it has declined and recovered according to our climatic assumption. The work by [21] presents evidence that during the

1960s, Ein Yotveta had a constant water flow at the surface. Given that this preceded our available data, we cannot attest to the changes that affected the vegetation during these years.

5. Conclusions

Nature conservation management, which aims to enhance ecological resilience while providing ecosystem services, must consider the climatic conditions and their effect on local ecosystems (Alcamo et al., 2003; Huang et al., 2020; Zhang et al., 2023). In this study, we coupled remote sensing imagery with rainfall data to estimate the changes that occurred in vegetation cover surrounding natural springs of the Arava during the last four decades. We estimated the responsiveness of vegetation to climatic conditions, and evaluated whether negative correlations were caused by human factors.

Our analysis implies that both the Senonian and the Quaternary aquifer-fed springs have responded to the prevailing multiyear rainfall conditions; vegetation cover has increased/ decreased during wet/dry sub-periods, respectively. We have identified that the Senonian aquifer springs are declining; there is a high negative correlation between vegetation cover and volumes of water extracted from the aquifer. The Quaternary (center) springs have been affected by anthropogenic activities as well, but mostly by water seepage from agricultural areas upstream, which increase vegetation cover. The statistical analysis of the Ein Yamluch spring emphasizes that all aquifer springs are at risk of drying if water extraction increases or during drier periods.

This paper offers a holistic approach to differentiate between the fluctuating climatic conditions and the anthropogenic impact to the vegetation cover around the natural springs of the Arava Valley. The insights drawn here can assist decision-makers to balance natural spring conservation and water extraction for human uses.

Acknowledgments: This research was supported by the Israel Nature and Parks Authority, the Hebrew University of Jerusalem Atid Scholarship, and the Department of Geography Gunther Scholarship, the Hebrew University of Jerusalem. We wish to thank Michelle Finzi for her editing assistance, we also wish to thank Arik Tzurilei, Prof. Hendrik Bruins, Ziv Sherzer, Mimi Ron, Roy Galili and Amnon Navon for sharing the data photos and insights.

Conflict of Interest Statement: The authors declare no conflicts of interest.

References

1. Morin, E. To Know What We Cannot Know: Global Mapping of Minimal Detectable Absolute Trends in Annual Precipitation: MINIMAL DETECTABLE PRECIPITATION TRENDS. *Water Resour. Res.* **2011**, *47*, doi:10.1029/2010WR009798.
2. Spinoni, J.; Micale, F.; Carrao, H.; Naumann, G.; Barbosa, P.; Vogt, J. Global and Continental Changes of Arid Areas Using the FAO Aridity Index over the Periods 1951-1980 and 1981-2010. **2013**, EGU2013-9262.
3. Bogan, M.T.; Noriega-Felix, N.; Vidal-Aguilar, S.L.; Findley, L.T.; Lytle, D.A.; Gutiérrez-Ruacho, O.G.; Alvarado-Castro, J.A.; Varela-Romero, A. Biogeography and Conservation of Aquatic Fauna in Spring-Fed Tropical Canyons of the Southern Sonoran Desert, Mexico. *Biodivers Conserv* **2014**, *23*, 2705–2748, doi:10.1007/s10531-014-0745-z.
4. Davis, J.A.; Kerezsy, A.; Nicol, S. Springs: Conserving Perennial Water Is Critical in Arid Landscapes. *Biological Conservation* **2017**, *211*, 30–35, doi:10.1016/j.biocon.2016.12.036.
5. Cartwright, J.M.; Dwire, K.A.; Freed, Z.; Hammer, S.J.; McLaughlin, B.; Misztal, L.W.; Schenk, E.R.; Spence, J.R.; Springer, A.E.; Stevens, L.E. Oases of the Future? Springs as Potential Hydrologic Refugia in Drying Climates. *Frontiers in Ecology and the Environment* **2020**, *18*, 245–253, doi:10.1002/fee.2191.
6. Hunter, M.L. Conserving Small Natural Features with Large Ecological Roles: An Introduction and Definition. *Biological Conservation* **2017**, *211*, 1–2, doi:10.1016/j.biocon.2016.12.019.
7. Wu, Q.; Bi, X.; Grogan, K.A.; Borisova, T. Valuing the Recreation Benefits of Natural Springs in Florida. *Water* **2018**, *10*, 1379, doi:10.3390/w10101379.
8. Danielopol, D.L.; Griebler, C.; Gunatilaka, A.; Notenboom, J. Present State and Future Prospects for Groundwater Ecosystems. *Environmental Conservation* **2003**, *30*, 104–130, doi:10.1017/S0376892903000109.
9. Luo, Q.; Yang, Y.; Qian, J.; Wang, X.; Chang, X.; Ma, L.; Li, F.; Wu, J. Spring Protection and Sustainable Management of Groundwater Resources in a Spring Field. *Journal of Hydrology* **2020**, *582*, 124498, doi:10.1016/j.jhydrol.2019.124498.

10. Parker, S.S.; Zdon, A.; Christian, W.T.; Cohen, B.S.; Palacios Mejia, M.; Fraga, N.S.; Curd, E.E.; Edalati, K.; Renshaw, M.A. Conservation of Mojave Desert Springs and Associated Biota: Status, Threats, and Policy Opportunities. *Biodivers Conserv* **2021**, *30*, 311–327, doi:10.1007/s10531-020-02090-7.
11. Ponder, W.F. Mound Springs of the Great Artesian Basin. In *Limnology in Australia*; De Deckker, P., Williams, W.D., Eds.; Monographiae Biologicae; Springer Netherlands: Dordrecht, 1986; pp. 403–420 ISBN 978-94-009-4820-4.
12. Evenari, M.; Shanan, L.; Tadmor, N.; Aharoni, Y. Ancient Agriculture in the Negev. *Science* **1961**, *133*, 979–996.
13. Whitcomb, D. The Misr of Ayla: Settlement at al-'Aqaba in the Early Islamic Period. *The Byzantine and Early Islamic Near East* **1994**, *2*, 155–170.
14. Yechieli, Y.; Reich, R.; Galili, E.; Tsuk, T.; Dahari, U.; Avni, G.; Sivan, D. Hydrogeology in Archeological Perspective: What Did People in Ancient Times Know About Hydrogeology? In *The Many Facets of Israel's Hydrogeology*; Kafri, U., Yechieli, Y., Eds.; Springer Hydrogeology; Springer International Publishing: Cham, 2021; pp. 417–443 ISBN 978-3-030-51148-7.
15. Chaimi, Y. *Ein Yahav- final report*; Hadashot Arkheologiyot: Excavations and Surveys in Israel; Israel Antiquities Authority, 2013;
16. Meshel, Z. A Fort at Yotvata from the Time of Diocletian. *Israel Exploration Journal* **1989**, *39*, 228–238.
17. Tucker, C.J.; Pinzon, J.E.; Brown, M.E.; Slayback, D.A.; Pak, E.W.; Mahoney, R.; Vermote, E.F.; El Saleous, N. An Extended AVHRR 8-km NDVI Dataset Compatible with MODIS and SPOT Vegetation NDVI Data. *International Journal of Remote Sensing* **2005**, *26*, 4485–4498, doi:10.1080/01431160500168686.
18. Groner, E.; Babad, A.; Berda Swiderski, N.; Shachak, M. Toward an Extreme World: The Hyper-Arid Ecosystem as a Natural Model. *Ecosphere* **2023**, *14*, e4586.
19. Kahana, R.; Ziv, B.; Enzel, Y.; Dayan, U. Synoptic Climatology of Major Floods in the Negev Desert, Israel. *International Journal of Climatology* **2002**, *22*, 867–882, doi:10.1002/joc.766.
20. Saaroni, H.; Halfon, N.; Ziv, B.; Alpert, P.; Kutiel, H. Links between the rainfall regime in Israel and location and intensity of Cyprus lows. *International Journal of Climatology* **2010**, *30*, 1014–1025, doi:10.1002/joc.1912.
21. Bruins, H.J.; Sherzer, Z.; Ginat, H.; Batarseh, S. DEGRADATION OF SPRINGS IN THE ARAVA VALLEY: ANTHROPOGENIC AND CLIMATIC FACTORS: DEGRADATION OF SPRINGS IN THE ARAVA VALLEY. *Land Degrad. Develop.* **2012**, *23*, 365–383, doi:10.1002/ldr.2149.
22. Rosenthal, E.; Adar, E.; Issar, A.S.; Batelaan, O. Definition of Groundwater Flow Patterns by Environmental Tracers in the Multiple Aquifer System of Southern Arava Valley, Israel. *Journal of Hydrology* **1990**, *117*, 339–368, doi:10.1016/0022-1694(90)90100-C.
23. Shentsis, I.; Rosenthal, E. Recharge of Aquifers by Flood Events in an Arid Region. *Hydrological Processes* **2003**, *17*, 695–712, doi:10.1002/hyp.1160.
24. Yechieli, Y.; Bein, A.; Burg, A.; Yarom, I. *The Impact of Flash Flood Interception on the Arava Shallow Groundwater: Characterization of the Interrelationships in the Natural and Disturbed Systems. Israel Geological Survey, Report TR-GSI/11/2001. 15 p. In Hebrew.*; 2001;
25. Frantzman, S.J.; Levin, N.; Kark, R. *Population, Space and Place*. May 27 2013,.
26. Al-Taani, A.A.; Rashdan, M.; Nazzal, Y.; Howari, F.; Iqbal, J.; Al-Rawabdeh, A.; Al Bsoul, A.; Khashashneh, S. Evaluation of the Gulf of Aqaba Coastal Water, Jordan. *Water* **2020**, *12*, 2125, doi:10.3390/w12082125.
27. Albalawneh, A.; Al-Assaf, A.; Sweity, A.; Hammour, W.A.; Kloub, K.; Hjazin, A.; Kabariti, R.; Abu Nowar, L.; Tadros, M.J.; Aljaafreh, S.; et al. Mapping Cultural Ecosystem Services in the Hyper Arid Environment of South of Jordan. *Frontiers in Environmental Science* **2022**, *10*.
28. McKee, T.B.; Doesken, N.J.; Kleist, J. THE RELATIONSHIP OF DROUGHT FREQUENCY AND DURATION TO TIME SCALES. **1993**, 6.
29. Vicente-Serrano, S.M.; Beguería, S.; López-Moreno, J.I. A Multiscalar Drought Index Sensitive to Global Warming: The Standardized Precipitation Evapotranspiration Index. *J. Climate* **2010**, *23*, 1696–1718, doi:10.1175/2009JCLI2909.1.
30. Kumar, M.N.; Murthy, C.S.; Sai, M.V.R.S.; Roy, P.S. On the Use of Standardized Precipitation Index (SPI) for Drought Intensity Assessment. *Meteorological Applications* **2009**, *16*, 381–389, doi:10.1002/met.136.
31. WMO *SPI: Standardized Precipitation Index*; european commission, 2013;
32. Aryee, J.N.A. Climate Indices/ SPI Calculation Available online: https://github.com/jeffjay88/Climate_Indices/blob/main/1D_spi_pandas.ipynb (accessed on 3 September 2023).
33. Ron, M.; Shalmon, B.; Alon, D.; Ramon, U. *The Arava - Nature and landscape survey*; Tel Aviv University: Deshe (OLI), 2003; p. 202;.
34. Dashora, A.; Lohani, B.; Malik, J.N. A Repository of Earth Resource Information – CORONA Satellite Programme. *Current Science* **2007**, *92*, 926–932.

35. Isaacson, S.; Blumberg, D.G.; Rachmilevitch, S.; Ephrath, J.E.; Maman, S. Using Remote Sensing and Spatial Analysis of Trees Characteristics for Long-Term Monitoring in Arid Environments. **2016**.
36. Houborg, R.; Mccabe, M. High-Resolution NDVI from Planet's Constellation of Earth Observing Nano-Satellites: A New Data Source for Precision Agriculture Available online: https://www.mdpi.com/2072-4292/8/9/768 (accessed on 20 September 2023).
37. Tucker, C.J. Red and Photographic Infrared Linear Combinations for Monitoring Vegetation. *Remote Sensing of Environment* **1979**, *8*, 127–150, doi:10.1016/0034-4257(79)90013-0.
38. Masek, J.G.; Vermote, E.F.; Saleous, N.E.; Wolfe, R.; Hall, F.G.; Huemmrich, K.F.; Gao, F.; Kutler, J.; Lim, T.-K. A Landsat Surface Reflectance Dataset for North America, 1990-2000. *IEEE Geoscience and Remote Sensing Letters* **2006**, *3*, 68–72, doi:10.1109/LGRS.2005.857030.
39. Vermote, E.; Justice, C.; Claverie, M.; Franch, B. Preliminary Analysis of the Performance of the Landsat 8/OLI Land Surface Reflectance Product. *Remote Sensing of Environment* **2016**, *185*, 46–56, doi:10.1016/j.rse.2016.04.008.
40. El Fellah, S.; Rziza, M.; El Haziti, M. An Efficient Approach for Filling Gaps in Landsat 7 Satellite Images. *IEEE Geosci. Remote Sensing Lett.* **2017**, *14*, 62–66, doi:10.1109/LGRS.2016.2626138.
41. Schmidt, H.; Karnieli, A. Remote Sensing of the Seasonal Variability of Vegetation in a Semi-Arid Environment. *Journal of Arid Environments* **2000**, *45*, 43–59, doi:10.1006/jare.1999.0607.
42. Siegal, Z.; Tsoar, H.; Karnieli, A. Effects of Prolonged Drought on the Vegetation Cover of Sand Dunes in the NW Negev Desert: Field Survey, Remote Sensing and Conceptual Modeling. *Aeolian Research* **2013**, *9*, 161–173, doi:10.1016/j.aeolia.2013.02.002.
43. Neeti, N.; Eastman, J.R. A Contextual Mann-Kendall Approach for the Assessment of Trend Significance in Image Time Series. *Transactions in GIS* **2011**, *15*, 599–611, doi:10.1111/j.1467-9671.2011.01280.x.
44. Venter, Z.S.; Barton, D.N.; Chakraborty, T.; Simensen, T.; Singh, G. Global 10 m Land Use Land Cover Datasets: A Comparison of Dynamic World, World Cover and Esri Land Cover. *Remote Sensing* **2022**, *14*, 4101, doi:10.3390/rs14164101.
45. Gutman, Y. *The center Arava region Updating the hydrological situation and recommendations for further development of Groundwater sources*; Mekorot- National Water Company, 2020; p. 88;.
46. Peleg, N.; Morin, E.; Gvirtzman, H.; Enzel, Y. Rainfall, Spring Discharge and Past Human Occupancy in the Eastern Mediterranean. *Climatic Change* **2012**, *112*, 769–789, doi:10.1007/s10584-011-0232-4.
47. Enzel, Y.; Bookman (Ken Tor), R.; Sharon, D.; Gvirtzman, H.; Dayan, U.; Ziv, B.; Stein, M. Late Holocene Climates of the Near East Deduced from Dead Sea Level Variations and Modern Regional Winter Rainfall. *Quaternary Research* **2003**, *60*, 263–273, doi:10.1016/j.yqres.2003.07.011.
48. Wu, X.; Liu, H.; Li, X.; Ciais, P.; Babst, F.; Guo, W.; Zhang, C.; Magliulo, V.; Pavelka, M.; Liu, S.; et al. Differentiating Drought Legacy Effects on Vegetation Growth over the Temperate Northern Hemisphere. *Global Change Biology* **2018**, *24*, 504–516, doi:10.1111/gcb.13920.
49. Zhao, A.; Yu, Q.; Feng, L.; Zhang, A.; Pei, T. Evaluating the Cumulative and Time-Lag Effects of Drought on Grassland Vegetation: A Case Study in the Chinese Loess Plateau. *Journal of environmental management* **2020**, *261*, 110214.
50. Krichak, S.O.; Alpert, P.; Krishnamurti, T.N. Interaction of Topography and Tropospheric Flow — A Possible Generator for the Red Sea Trough? *Meteorl. Atmos. Phys.* **1997**, *63*, 149–158, doi:10.1007/BF01027381.
51. Drori, R.; Ziv, B.; Saaroni, H.; Etkin, A.; Sheffer, E. Recent Changes in the Rain Regime over the Mediterranean Climate Region of Israel. *Climatic Change* **2021**, *167*, 15, doi:10.1007/s10584-021-03161-6.
52. Enmar, L. *The travertines in the northern and central Arava: stratigraphy, petrography and geochemistry.*; Geological Survey of Israel: Jerusalem (, 1999;
53. Oren, O.; Yechieli, Y.; Böhlke, J.K.; Dody, A. Contamination of Groundwater under Cultivated Fields in an Arid Environment, Central Arava Valley, Israel. *Journal of Hydrology* **2004**, *290*, 312–328, doi:10.1016/j.jhydrol.2003.12.016.
54. Shalev, N.; Burg, A.; Gavrieli, I.; Lazar, B. Nitrate Contamination Sources in Aquifers Underlying Cultivated Fields in an Arid Region – The Arava Valley, Israel. *Applied Geochemistry* **2015**, *63*, 322–332, doi:10.1016/j.apgeochem.2015.09.017.
55. Zurieli, A. *Current Hydrogeological Situation to the Northern Prairie Area and Sodom Square*; The hydrological service: Jerusalem, 2016;